

Graphene Oxide-TiO₂ composite as a novel adsorbent for the preconcentration of heavy metals and rare earth elements in environmental samples followed by on-line inductively coupled plasma optical emission spectrometry detection

Yanan Zhang, Cheng Zhong, Qiangying Zhang, Beibei Chen, Man He*, Bin Hu

Key Laboratory of Analytical Chemistry for Biology and Medicine (Ministry of Education),
Department of Chemistry, Wuhan University, Wuhan 430072, China

Supplementary Information

Fig. S1. FT-IR spectra of GO (A), TiO₂ (B) and GO-TiO₂ (1:1) (C).

Fig. S2. TGA of GO (A) and GO-TiO₂ (1:1) composite (B); DTG of GO (C) and GO-TiO₂ (1:1) composite (D).

Fig. S3. XRD pattern of GO (A), TiO₂ (B) and GO-TiO₂ (1:1) composite (C).

Fig. S4. Effect of 1 mol L⁻¹ HNO₃ volume on the recovery of the analytes. pH: 5; The concentration of the metal ions: 0.5 μg mL⁻¹; Sample volume: 2.5 mL; Flow rate: 0.5 mL min⁻¹

Fig. S5. Effect of elution flow rate on recovery of the analytes. pH: 5; The concentration of the metal ions: 0.5 μg mL⁻¹; Sample volume: 2.5 mL; Sample flow rate: 0.5 mL min⁻¹; Eluent concentration: 1 mol L⁻¹ HNO₃; Eluent volume: 0.7 mL

Fig. S6. Effect of sample volume on recovery of the analytes. pH: 5; The absolute concentration of each metal ion: 1.25 μg; Sample flow rate: 2.0 mL min⁻¹

Fig. S7. Breakthrough curves of GO-TiO₂ (1:1) of the analytes. (10 μg mL⁻¹ at a sample flow rate of 2.0 mL min⁻¹)

Table S1. Comparison of adsorption capacities (mg g⁻¹) with those reported in the literature

Table S2. Correlation coefficient values of the Pseudo-first-order and Pseudo-second-order

Table S3. Comparison of the method with those reported in the literature (on-line SPE-ICP-OES)

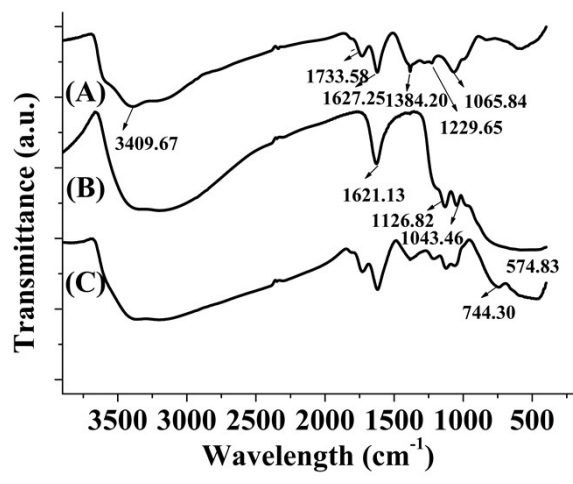


Fig. S1.

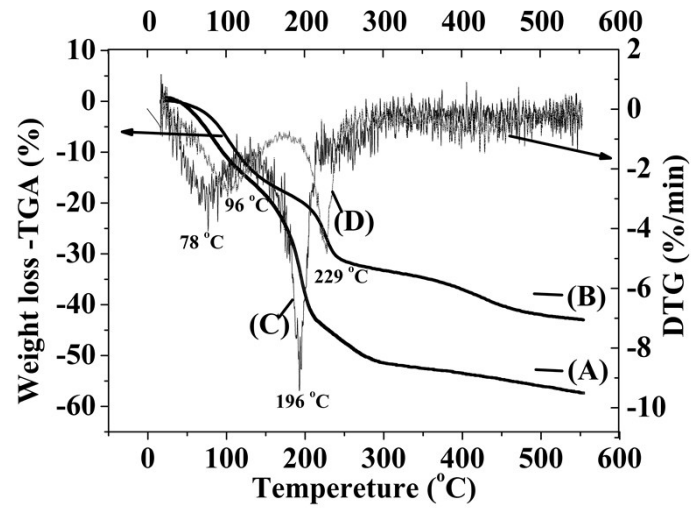


Fig. S2.

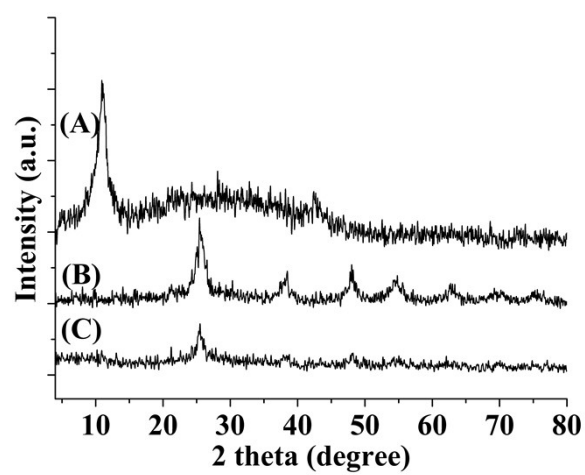


Fig. S3.

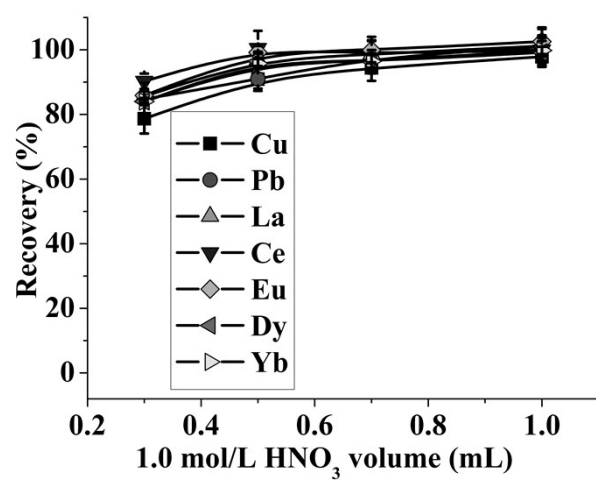


Fig. S4.

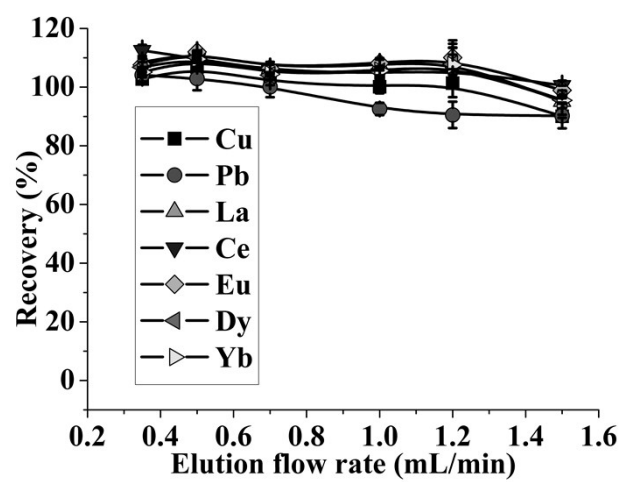


Fig. S5.

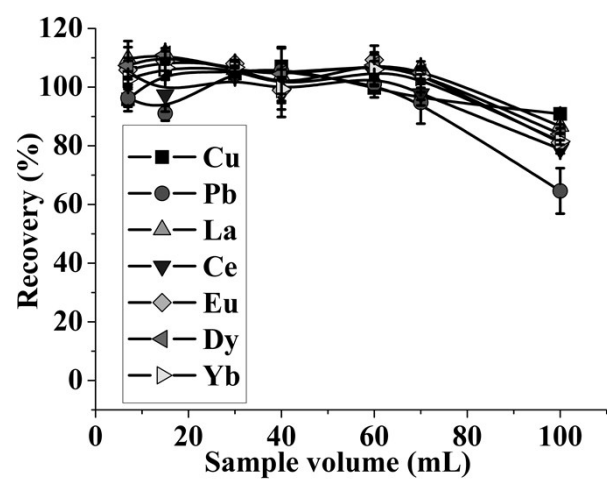


Fig. S6.

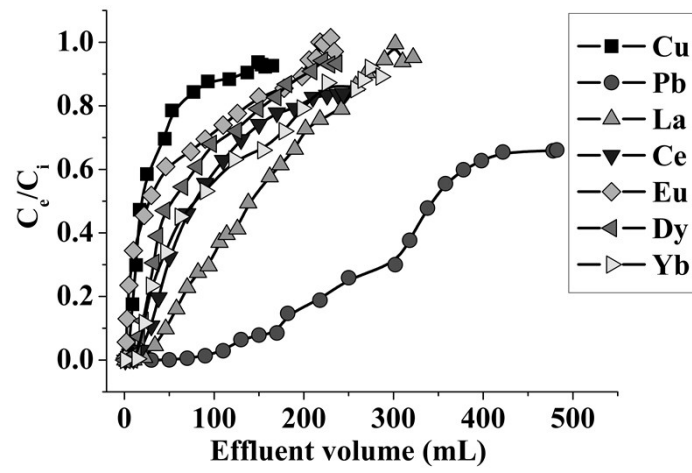


Fig. S7.

Table S1.

Materials	Cu	Pb	La	Ce	Eu	Dy	Yb	Ref.
nanometer-sized TiO ₂	—	—	7.0	—	8.3	8.8	9.8	13
modified mesoporous TiO ₂	11.7	17.7	—	—	—	—	—	11
mesoporous TiO ₂	8.1	—	21.3	13.8	19.5	16.7	26.5	12
PAN-modified nano-TiO ₂	4.73	—	—	—	—	—	6.14	15
Graphene (dithizone)	—	16.6	—	—	—	—	—	21
MWNTs	—	—	8.30	—	9.43	—	8.57	19
MWCNT-PPy	—	25	—	—	—	—	—	20
TiO ₂ Nanotubes	—	—	12.3	10.1	13.2	—	14.7	37
oxidized SWNTs	5.4	6.2	—	—	—	—	—	18
GO@SiO ₂	6.0	13.6	—	—	—	—	—	33
GO-TiO ₂	8.2	64.2	28.7	25.1	16.6	19.3	24.1	This work

Table S2.

Analyte	Pseudo-first-order			Pseudo-second-order		
	R_A^2	R_C^2	R_E^2	R_B^2	R_D^2	R_F^2
Cu	0.892	0.999	0.937	0.996	0.991	0.999
Pb	0.802	0.988	0.839	0.907	0.860	0.994
La	0.832	0.998	0.815	0.984	0.935	0.999
Ce	0.785	1.000	0.761	0.994	0.968	0.999
Eu	0.772	0.999	0.820	0.971	0.964	0.990
Dy	0.831	0.997	0.856	0.981	0.977	0.997
Yb	0.876	0.999	0.841	0.998	0.995	0.996

Table S3.

Materials	Sample throughput (h ⁻¹)	Enrichment factor	LODs (ng mL ⁻¹)							Ref.
			Cu	Pb	La	Ce	Eu	Dy	Yb	
nanometer-sized TiO ₂	—	50	—	—	0.36	—	0.12	0.28	0.10	13
nanometer-sized TiO ₂	—	50	0.34	—	—	—	—	—	—	14
modified mesoporous TiO ₂	10	20	0.23	0.50	—	—	—	—	—	11
mesoporous TiO ₂	20	10	0.12	—	0.16	0.35	0.07	0.10	0.03	12
PAN-modified nano-TiO ₂	—	5	2.8	—	—	—	—	—	0.6	15
activated carbon	29	30	0.1	—	—	—	—	—	—	48
GO-TiO ₂	12	10	0.48	2.64	0.41	0.24	0.13	0.26	0.21	This work